INTERNAL SOLITARY WAVE PROPAGATION IN ICE-COVERED WATER

Magda Carr (1), Andrea Haase (2), Karl-Ulrich Evers (3), Ilker Fer (4), Peter Sutherland (5), Atle Jensen (6), Henrik Kalisch (4), Jarle Berntsen (4), Emilian Părău (7), Øyvind Thiem (8) & Peter. A. Davies (9)

(1) Newcastle University, UK, E-mail: magda.carr@ncl.ac.uk
(2) Hamburg Ship Model Basin, Germany, E-mail: Haase@hsva.de
(3) Solutions4Arctic, Hamburg, Germany, Email: kueham@gmail.com
(4) University of Bergen, Norway, E-mail: ilker.fer@uib.no henrik.kalisch@uib.no jarle.berntsen@uib.no
(5) IFREMER, University of Brest, France, E-mail: peter.sutherland@ifremer.fr
(6) University of Oslo, Norway, E-mail: atlej@math.uio.no
(7) University of East Anglia, UK, E-mail: e.parau@uea.ac.uk
(8) Norwegian Public Roads Administration, Bergen, Norway, E-mail: oyvind.thiem@vegvesen.no
(9) University of Dundee, UK, E-mail: p.a.davies@dundee.ac.uk

Internal solitary waves (ISWs) propagating in a stably-stratified two layer fluid in which the surface condition changes from open water to different ice types namely, nilas ice, grease ice and level ice are studied. Experiments are conducted in a cold laboratory at the Hamburg Ship Model Basin (HSVA). A customized flume is designed and built. Specific objectives are to obtain accurate measurements of (i) wave amplitude, (ii) wave-induced velocity field, and (iii) wave speed. In addition, measurements of ice thickness and wave-induced ice floe speed are made. The main questions to address are (i) what is the dissipation of ISW energy under different ice conditions and (ii) what is the effect of ISW energy on the ice dynamics?

1. INTRODUCTION

Oceanic internal solitary waves (ISWs) propagate along density interfaces and are ubiquitous in stratified water. Their properties are strongly influenced by the nature of the sea surface above the waves, and by the geometry of the containing basin below. As the Arctic Ocean evolves to a seasonally more ice-free state, the internal wave field will be affected by the changes at the surface. The relationship between ISW dynamics and ice is crucial in understanding (i) the general circulation and thermodynamics in the Arctic Ocean and (ii) local mixing processes that supply heat and nutrients from depth into upper layers, especially the photic zone. This, in turn, has important ramifications for sea ice formation processes and the state of local and regional ecosystems.

It is known that ISWs cause flexure of sea ice (Czipott *et al*., 1991; Marchenko, Morozov, Muzylev, & Shestov, 2010) and theoretical studies suggest that they are responsible for the formation of ice bands in the marginal ice zone. However, the effect of diminishing sea ice cover on the ISW field (and vice versa) is not well established. A better understanding of ISW dynamics in the Arctic Ocean and, in particular, how the ISW field is affected by changes in both ice cover and stratification, is central in understanding how the rapidly changing Arctic will adapt to climate change.

While field observations have provided insight into ISW dynamics in the Arctic Ocean, none to date isolate the effects of individual ice, ocean and wind parameters. Satellite imagery has provided valuable new insight but its use is restricted to areas of open water and to climatic conditions being favourable for the observations to be made. There is a clear need, therefore, to supplement field work with modelling studies. In this campaign, a laboratory investigation of ISWs in a two-layer stratified flow propagating from open water to under different ice features is performed. The ice type is varied and the interaction between the ISW and ice investigated. This is the first time that ISWs have been generated under ice in a laboratory setting.

This paper presents the experimental set-up, the model ice production and some key findings. The data processing and data analysis is under review in *Geophysical Research Letters* (Carr *et al.*, 2019).

2. EXPERIMENTAL SET UP AND PROCEDURE

2.1 GENERAL DESCRIPTION

The experiments were performed in the Arctic Environmental Test Basin (AETB) at the Hamburg Ship Model Basin (HSVA). The AETB is a cold room which houses a basin of 30m length, 6m width and 1.5m depth and has a volume of 270m^3. The room can be cooled to a temperature of -15°C. For this study, the basin was emptied and an internal wave flume was designed and custom-built within the AETB. The wave flume had dimensions of 6m in length, 0.5m in width and 0.6m in depth and consisted of rectangular aluminium profiles (type Bosch-Rexroth 45/45; 90/90 and 90/180mm) with corner connections and 15 mm thick transparent Plexiglass® plates (*Fig. 1*). The Flume was composed of 2 Plexiglass® elements (length=3000m, width=470mm and height=600mm) which had a total length of 6000mm and was based on a foundation that also consisted of rectangular aluminium profiles (12 supports). The Plexiglass® construction allowed visualisation from the side and illumination from below. The total height of the experimental set-up was approximately 1.7m.

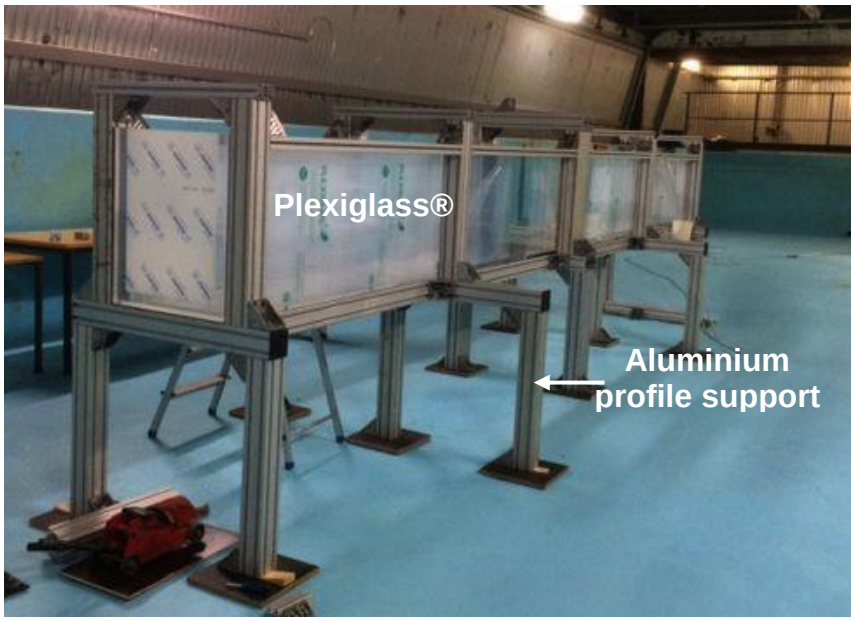

Figure 1. Plexiglass® flume (6m x 0.47m x 0.6m) installed within HSVA's (blue) Arctic Environmental Test Basin.

2.2 STRATIFICATION OF THE WATER COLUMN

The flume was filled with homogeneous salt water of prescribed density ρ_3 = 1045 kg/m^3 to a depth h_3. Less dense brine solution of density ρ_1 = 1025 kg/m^3 was then slowly added to the top of the dense salt water layer via an array of floating surface sponges (*Fig. 2*). Consequently, an interface (pycnocline) between the two fluids formed in which the density, varied as a linear function of depth *z*. After the flume was stratified, ice was then made or added at the surface such that half the surface was ice-covered and the other half was ice-free. *Figure 3* shows a schematic diagram of the flume arrangement.

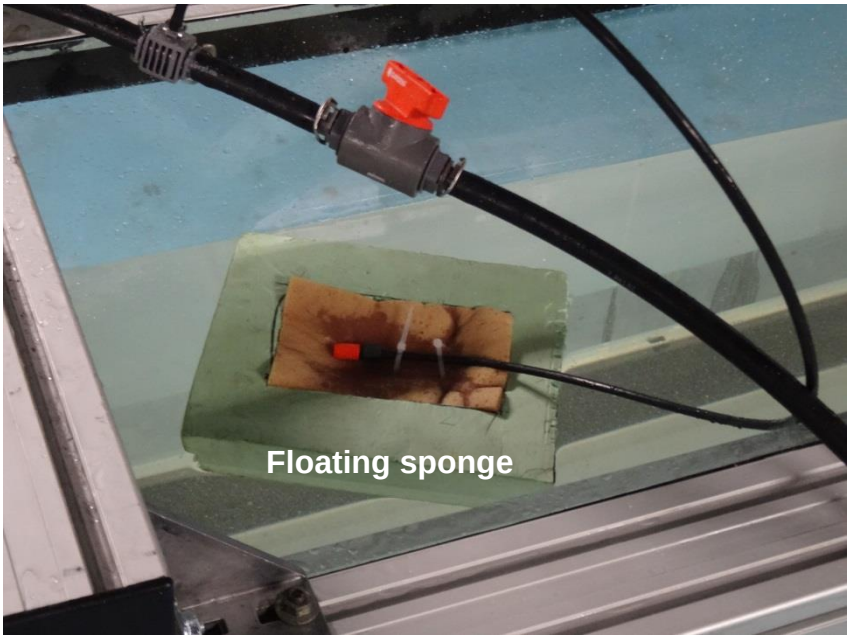

Figure 2. Brine solution of density ρ_1 = 1025 kg/m^3 was added via an array of floating surface sponges.

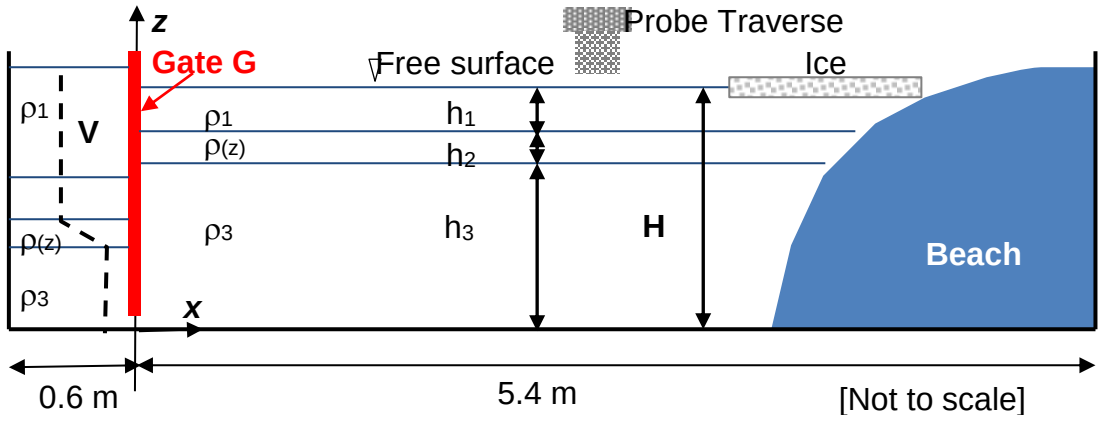

Figure 3. Schematic diagram of the flume arrangement.

2.3 ICE PRODUCTION

Different ice types were frozen on the surface of the water column or produced in the Large Ice Model Basin (LIMB) at HSVA and then added to the water surface in the flume.

(i) **Level ice** was made in the LIMB. The model level ice was frozen from a 0.7% sodium chloride solution in the natural way, i.e. the water/ice surface was exposed to cooled air. The preparation of the ice sheet was started by a seeding procedure. For this purpose water was sprayed into the cold air of the ice tank. The droplets froze in the air forming small ice crystals which settled on the water surface. By this method the growth of a fine-grained ice of primarily columnar crystal structure was initiated. Tank water which had been pressure-saturated with air was uniformly discharged along the tank bottom during the entire freezing process. Immediately after discharging, the surplus air segregated from the water and formed tiny air bubbles. These air bubbles whose diameter ranged from 200−500 microns rose to the ice sheet, where they were

embedded into the growing ice crystals. An advantage of the air content in the ice is the possibility to adjust the ice density so that the density difference between ice and water is within the natural range. The embedded air bubbles gave the model ice a white appearance (Evers & Jochmann (1993); Evers, 2015). When the ice sheet reached a certain thickness, sections were cut and removed from the LIMB, and then kept in a cold storage unit on boards of wood until required. The floes of level ice, sitting on wood, were carefully lowered into the stratification and then the wood slid out from beneath them (*Fig. 4*).

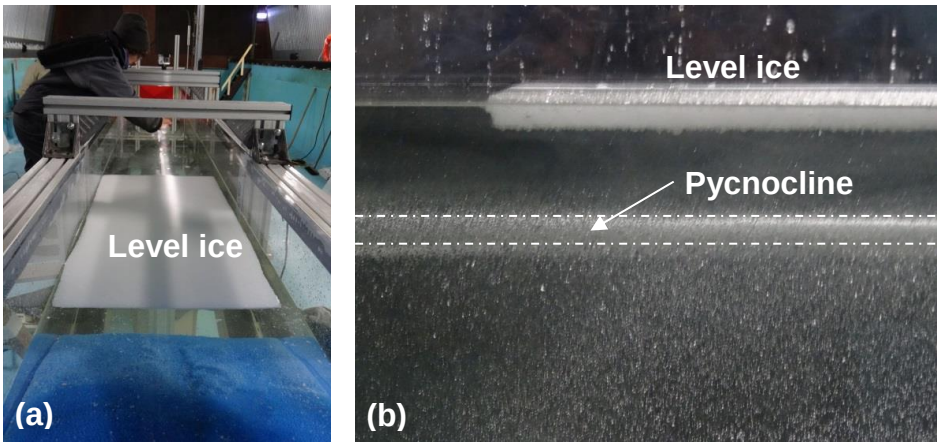

Figure 4. Level ice floe in the stratified flume (a) viewed from above and (b) viewed from the side; the pycnocline is shown in (b).

(ii) **Grease ice/brash ice** was made in buckets by crushing model level ice. The grease ice was then carefully added to the surface of the water column using a grate and hand shovel (*Fig. 5*). The grate was placed in the top layer of the water column; care was taken not to disturb the pycnocline and the grease ice was slowly poured over the grate using the hand shovel. The grate was then removed from the water column.

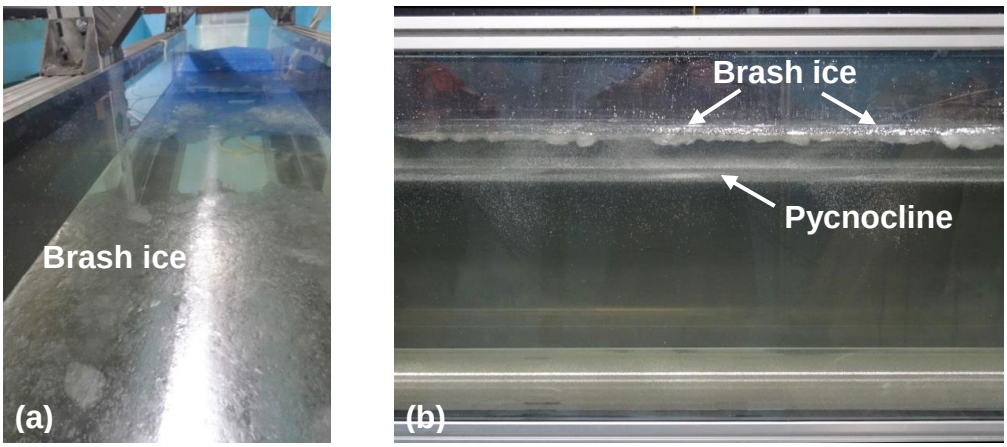

Figure 5. Brash/Grease ice in the stratified flume (a) viewed from above and (b) viewed from the side; the pycnocline is shown in (b).

(iii) **Nilas ice** was made by reducing the temperature in the AETB so that the surface of the water column in the flume froze (*Fig. 6*). Open water sections were maintained by placing styrofoam at the surface during the freezing process. The styrofoam lids were removed just prior to an experiment commencing.

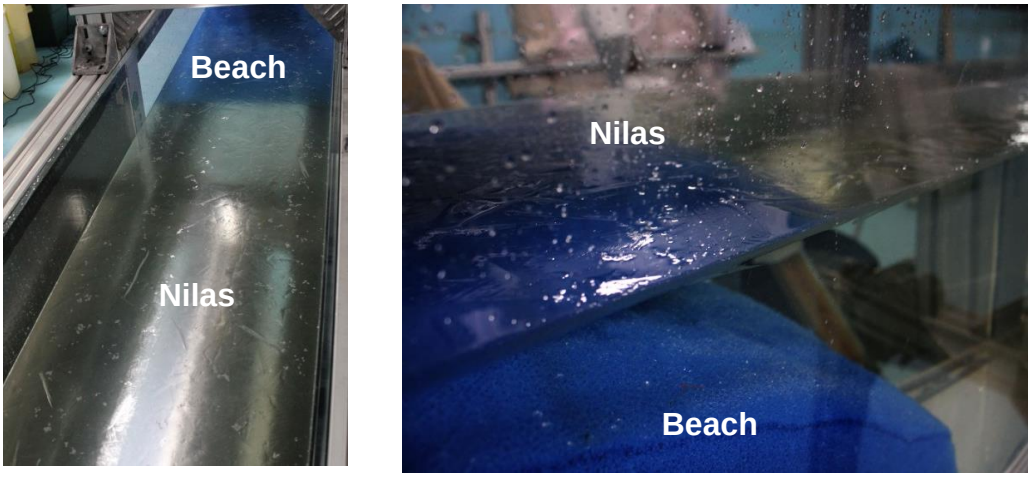

Figure 6. Nilas ice in the stratified flume.

A gate was inserted at the upstream end of the flume (*Fig. 7a*) and lowered approximately 1 cm above the bottom of the flume. A beach consisting of polyether filter foam (*Fig. 7b*) was placed at the downstream end of the flume and absorbed some of the ISW energy. A fixed Volume *V*, of water density ρ_1 was then added behind the gate. Due to hydrostatic balance, fluid of density ρ_3 flowed under the gate into the main section of the flume. After the Volume, *V*, was added, the entire fluid depth H, in the main section of the flume was measured using a pre-set tape on the Plexiglass® window. During filling the air temperature was kept just above *T*= 0°C.

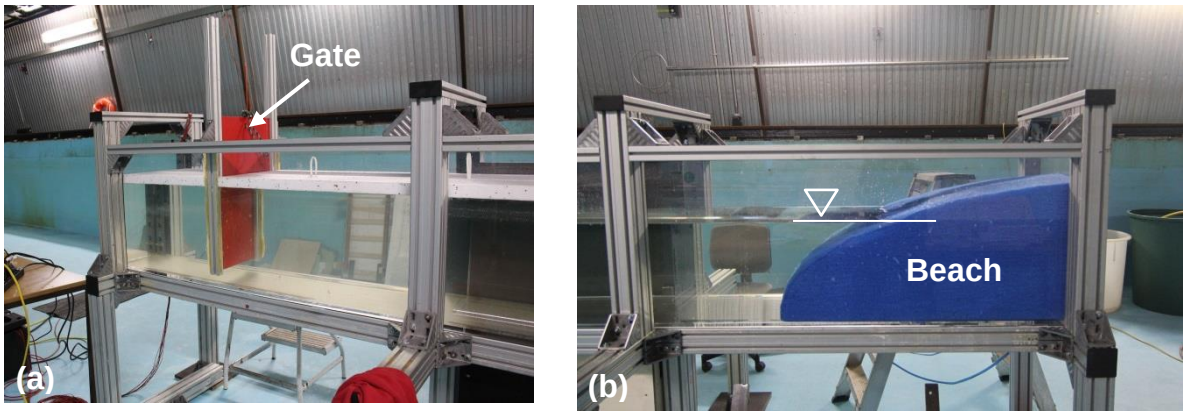

Figure 7. Arrangement of (a) gate and (b) beach within the flume.

2.4 WAVE GENERATION

ISWs were generated by removal of the gate which was lifted quickly and smoothly in the vertical direction. After a sorting distance of about 1 m, an ISW of depression propagated along the pycnocline into the main section of the flume. Once an experiment was finished and the water column stationary, the gate, was reinserted and a fixed volume of fluid of density ρ_1 was again added behind the gate so that a second (and sometimes third) wave could be generated.

2.5 FLOW MEASUREMENT AND VISUALISATION

The stratification was measured using MSCTI high precision micro-conductivity sensors (Precision Measurement Engineering). The sensors were mounted on a rigid rack and pinion traverse system fitted with a potentiometer. The sensors were moved vertically through the water

column and density profiles were obtained by calibrating the potentiometer output and conductivity data against known values of height and fluid density respectively. The micro-conductivity probes sampled at 10 k Hz and profiles were acquired just prior to a given experimental run commencing.

A light source (intensive LED strip passing through a double slit) was placed beneath the transparent base of the flume. This generated a thin vertical column of light illuminating a 2D-slice of the flow field in the mid-plane of the flume. In order to make the streamlines of the flow visible, the water column was seeded with neutrally-buoyant, light-reflecting tracer particles of "Pliolite" having grain diameter in the range 150 – 300 microns.

Three UNIQ UP-1830CL-12B 2/3" 1024 x 1024 Mono 12 bit digital cameras attached to R64-PCE-CL-D R64e PCI Express frame grabbers were used to record the fluid motion. The cameras were set up outside of the flume and viewed the flow field orthogonally from the side. Video capture took place throughout an experiment. The cameras were arranged so that they had overlapping fields of view and a light source was used such that the cameras were synchronised in time (*Fig. 8a*). The *UNIQ* cameras sampled at 30 frames a second.

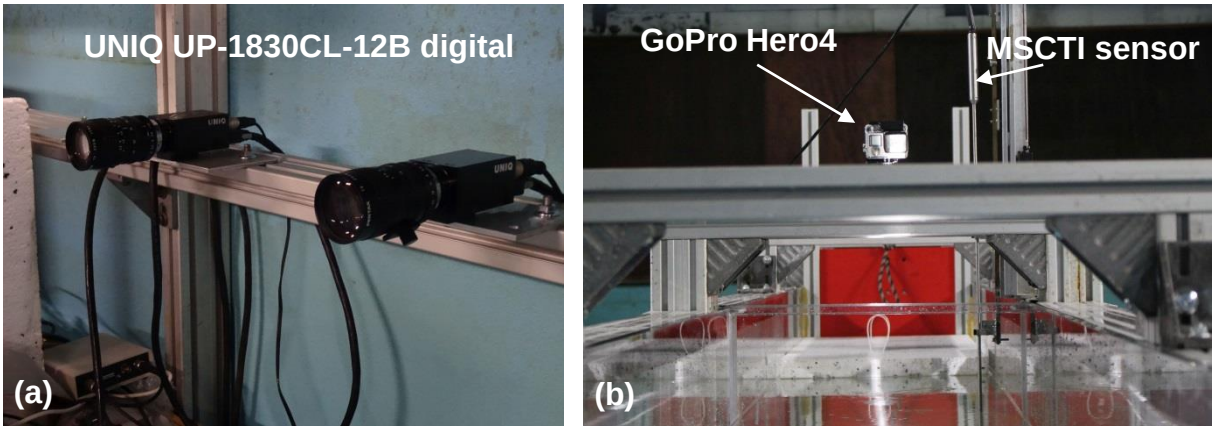

Figure 8. The photo shows (a) 2 of the 3 UNIQ cameras used and (b) the position of the *GoPro Hero 4* camera and the *MSCTI* conductivity sensor.

The video records were processed using the software package *DigiFlow*. From the time series function of *DigiFlow* the wave speed, wave amplitude, wave length and wave-induced ice floe speed were measured. The PIV-function of *DigiFlow* was used to calculate continuous synoptic velocity and vorticity field data along the illuminated cross-section in the middle part of the flume.

A *GoPro Hero 4* camera was set up above the flume (just upstream of the ice edge) and viewed the surface of the water column from above (*Fig. 8b*).

2.6 ICE AND TEMPERATURE MEASUREMENTS

Calipers were used to determine ice thickness. To measure the temperature and the salinity of the water in the reservoirs before and during the experiment a Type *WTW Multi 3310 IDS* device equipped with a conductivity cell of type *WTW TetraCon 925* was used. To measure ice core temperature a thermometer of type *Testo 720* was used and a generic hydrometer was used to measure the density of the water.

The room temperature at different locations of the AETB was recorded continuously during the campaign as was water temperature in the flume by means of a *PT100* sensor chain. A photo of the arrangement is given in *Figure 9.*

Channel	Height above base of flume [mm]
Ch 1 Ch 2	550 (air) 500 (air)
Ch 3	425 (air, sometimes water)
Ch 4 Ch 5	375 (water usually top layer) 275 (water usually bottom layer)
Ch 6 Ch 7 Ch 8	175 (water bottom layer) 100 (water bottom layer) 50 (water bottom layer)

Figure 9. *PT 100* sensor arrangement

Ice was sampled from the flume and the ice density was determined. The results from a given test day (18-04-2018) are summarized in *Table 3.*

Table 3. Results of ice density measurements

Run [-]	Length L [m]	Breadth B [m]	Thickness H [m]	Weight G [kg]	Volume V $1*10^{-04}$ [m3]	Density ρ_{ice} [kg/m3]
1	0.098	0.089	0.014	0.980	1.22108	803
2	0.098	0.100	0.015	0.115	1.47000	782

3. EXPERIMENTAL PROGRAMME

Table 4 provides a summary of the experimental runs. “Date” is the date of the experiment, “Run” is the run number for a given day, “Ice type” provides a summary of the ice type, “h3”, “h2”, “h1” are the stratification layer thicknesses. H is the total fluid depth and V is the wave generating volume of fluid added behind the gate.

Table 4. Experimental programme. “h3”, “h2”, “h1” are the stratification layer thicknesses, “H” is the total fluid depth and “V” is the wave generating volume of fluid added behind the gate.

Date	Run	Ice type	h_3	h_2	h_1	H	V
[ddmmyyyy]	[-]	[-]	[mm]	[mm]	[mm]	[mm]	[$1*10^6$ mm^3] resp. litres
10-04-2018	1	Nilas smooth & thin - whole surface covered	322	35	43	399	31
	2	Nilas thick & rough - wholesurface covered	307	37	68	412	31
	3	Grease - whole surface covered	276	57	90	424	31
12-04-2018	1	Grease - surface partially covered	323	31	44	399	31
	2	Grease - surface partially covered	330	35	55	420	60
17-04-2018	1	Nilas - surface partially covered but fixed in x	321	35	44	400	31
	2		332	30	57	420	60
18.04.2018	1	Thin level ice - surface partially covered, free to move	316	38	47	401	30
	2		323	42	55	421	60
19-04-2018	1	Thick level ice - surface partially covered, free to move	302	60	45	406	31
	2		314	59	53	426	61
	3	Thick level ice and double length	313	56	83	452	60

4. MAIN RESULTS

The experiments showed that the ISW-induced flow at the surface was capable of transporting ice floes in the horizontal direction. It is anticipated that the results will allow the transport speed of the ice to be parameterised in terms of the wave induced horizontal velocity, the wave length, the floe thickness, the floe ice type and the floe length respectively.

In thick ice cover cases, in which the thickness of the ice was comparable to the depth of the top layer in the stratification, the ice significantly damped the ISW signal causing the wave to break and even be destroyed in some cases.

The roughness associated with different ice types caused varying degrees of vorticity and turbulence in the wave-induced boundary layer beneath the ice. It is hoped that the velocity data

obtained (via PIV) can be used to analyse wave dissipation rates for different wave properties and ice types.

5. CONCLUSION

The objective of the study was to generate ISWs under different ice types, namely, nilas, grease, and level ice. The main focus of the experiments was to (i) obtain accurate measurements of the wave induced velocity field under the ice and (ii) get a qualitative understanding of how different ice conditions affect the ISW field.

ISWs were generated using a sluice gate and the surface condition was varied. Measurements of wave speed, wave amplitude and wave induced velocity under the ice were obtained in the mid-plane of the tank. Difficulties in visualisation very close to the bottom side of the ice were encountered due to (i) reflection of the light source off the underside of the ice and (ii) ice at the front of the tank obstructing the field of view.

The range of investigated parameters was limited by the duration of the experimental campaign and the scale of the flume. The experiments are original and unprecedented; combining stratified ISW flow with ice.

Preliminary results and observations indicate the need for further more detailed investigations and show clearly that the physical interactions of ISWs with ice have significant implications for ISW energy dissipation and mixing processes in polar oceans.

ACKNOWLEDGEMENT

This project has received funding from the European Union's Horizon 2020 research and innovation programme under grant agreement No 654110, HYDRALAB+. This work received funding from the MASTS pooling initiative (The Marine Alliance for Science and Technology for Scotland) and their support is gratefully acknowledged. MASTS is funded by the Scottish Funding Council and contributing institutions. The authors thank Gesa Ziemer and Nis Schnoor for providing technical assistance at HSVA, Hamburg.

REFERENCES

Carr, M., Haase, A., Evers, K.-U., Fer, I., Sutherland, P., Jensen, A., Kalisch, H., Berntsen, J., Părău, E., Thiem, Ø. and Davies, P. A. (2019). Laboratory Experiments on Internal Solitary Waves in Ice-Covered Waters. *Submitted to American Geophysical Union (AGU) - Geophysical Research Letters*

Czipott, P.V., Levine, M.D., Paulson, C.A, Menemenlis; D., Farmer, D.M, & Williams, R.G. (1991). Ice flexure forced by internal wave packets in the Arctic Ocean. *Science*, 254, 832-835.

Evers, K.-U., Haase, A. and Carr, M. (2019). Physical experiments of internal solitary waves (ISWs) under various ice conditions in a cold laboratory, Proceedings 25th International Conference on Port and Ocean Engineering under Arctic Conditions, Delft, The Netherlands, 9 – 13 June 2019, *submitted to POAC on March 15, 2019*

Evers, K.-U. (2015). Modeling ice processes in laboratories and determination of model ice properties. In P. Langhorne (Ed.), Cold regions science and marine technology. EOLSS Publishers

Evers & Jochmann (1993). An Advanced Technique to Improve the Mechanical Properties of Model Ice Developed at the HSVA Ice Tank. Proceedings POAC'93

Marchenko, A.V., Morozov, E., Muzylev, S.V., & Shestov, A.S. (2010). Interaction of short internal waves with ice cover in an Arctic fjord. *Oceanology, 50,* 18-27